

LETTER | JUNE 15 1989

Evaporation of small water drops maintained at constant volume

Clarence N. Peiss



J. Appl. Phys. 65, 5235–5237 (1989)

<https://doi.org/10.1063/1.343165>



Articles You May Be Interested In

Scanning tunneling microscope imaging technique for weakly bonded surface deposits


J. Appl. Phys. (June 1989)

Influence of Irradiation with β Rays on the Electrification of KCl Crystals

J. Appl. Phys. (March 1960)

Evaporation of drops containing active colloids

AIP Conf. Proc. (August 2024)



Journal of Applied Physics

Special Topics Open for Submissions

[Learn More](#)

Evaporation of small water drops maintained at constant volume

Ciarence N. Peiss^{a)}

Department of Physiology, Loyola University Stritch School of Medicine, Maywood, Illinois 60153

(Received 13 December 1988; accepted for publication 20 February 1989)

An apparatus was devised which permits measurement of the evaporative rate of small water drops maintained at constant volume. The surface temperature of the drop was measured with a small thermocouple. Evaporative rates were measured at drop radii ranging from 0.023 to 0.18 cm, with a total of 128 measurements. Mathematical analysis was performed using a multiple curve fitting program for 19 different curves. It was found that a plot of radius against evaporative rate (g/s/mm Hg) is best fit by a parabola with a correlation coefficient of 0.998.

The rate of evaporation of a water drop can be expressed by an equation derived from Stefan's¹ general theory of diffusion:

$$V = 4\pi rD \log_e [(P - P_a)/(P - P_s)], \quad (1)$$

where V is the evaporative rate in cc water vapor per second, P is the barometric pressure, P_a is the vapor pressure of the air, P_s is the saturation vapor pressure at the surface of the water drop, r is the radius of the drop and D is the diffusion coefficient. When the evaporative rate (E) is expressed in grams per second, and when $P_a = 0$, this equation becomes

$$E = 0.0101rD \log_e [P/(P - P_s)]. \quad (2)$$

When P_s is small with respect to total pressure and within the temperature range of the experiments reported here, Eq. (2) gives values almost identical with those calculated from Langmuir's² equation:

$$\frac{dm}{dt} = 4\pi rD \frac{MP_s}{RT}, \quad (3)$$

where M is the molecular weight of water, R is the gas constant, and T is the absolute temperature. These equations postulate that the evaporative rate of a sphere is proportional to the radius of the sphere, and several prior studies³⁻⁶ indicated approximate agreement with this postulate. There are several experimental problems with many prior studies. If the range of sphere radii is small, the data for evaporative rate may appear to be linear with respect to radius. In other cases, mathematical analysis shows that the data are best fit by a curve other than linear. In most other studies, the temperature of the sphere's surface has not been measured, so that it was not possible to determine surface vapor pressure and thus express the data in terms of evaporative rate per mm Hg vapor pressure. Moreover, recording surface temperature usually causes distortion of the sphere as the water drop decreases in size.

An experimental method was devised with which it was possible to measure the evaporative rate of a water drop maintained at constant volume (isovolumic evaporation), and to record surface temperature continuously. This procedure was used to measure evaporative rates over a fairly wide range of drop diameters.

Figure 1 is a schematic diagram of the experimental ap-

paratus. The drop of distilled water was formed on a blunt-end hypodermic needle within a closed Plexiglass chamber. Several needle diameters were used, depending on the size of the water drop being measured. Measured evaporative rates were corrected for the partial area of the drop occupied by the needle, so that the rates shown in Fig. 2 are for the full sphere. Air vapor pressure was kept at 0-mm Hg by using a layer of Drierite in the bottom of the chamber. Air and water drop surface temperatures were measured with thermocouples (TC_a , TC_w), the latter having a junction diameter of 0.075 mm. Temperature readings were made with a Fluke Model 2190A Digital Thermometer accurate to 0.1 °C. A typical experiment was of 20-min duration. After a water drop was formed on the needle, it was allowed to sit for 10 min at constant volume. During this time the drop temperature equilibrated to a level of 12–15 °C depending on drop size. Measurement of evaporative rate was then made for another 10-min period, during which drop temperature either remained constant or decreased by 0.1 °C. Air and bulk water temperatures were in the range of 19–22 °C and did not vary more than 0.1 °C during the measurement period.

Water drop diameter was measured with a Microcode Digital Reading Optical Micrometer attached to one eyepiece of a Nikon Stereozoom microscope. Drop size was kept constant by injecting water into the drop through the hypodermic needle at the same rate at which the drop was evaporating. This was accomplished by a servo device which controlled an Inchworm apparatus. A glass capillary microelectrode (GME) with a tip diameter of 1 μm or less was filled with 3M KCl solution. The microelectrode and the water drop thermocouple were mounted in micromanipula-

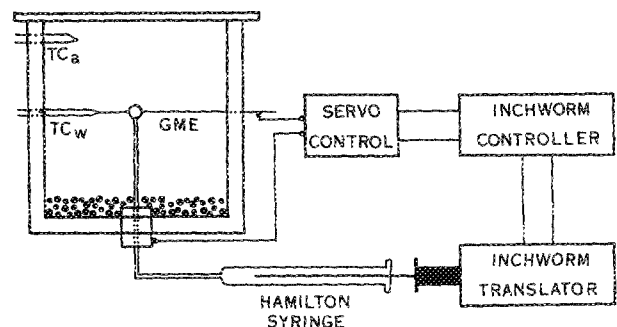


FIG. 1. Schematic diagram of apparatus for measurement of evaporation of water drops maintained at constant volume. TC = thermocouple. GME = glass microelectrode.

^{a)} Professor and Dean Emeritus. Present address: 360 E. Randolph Dr., Apt. 1507, Chicago, IL 60601. Reprint requests to the Department of Physiology.

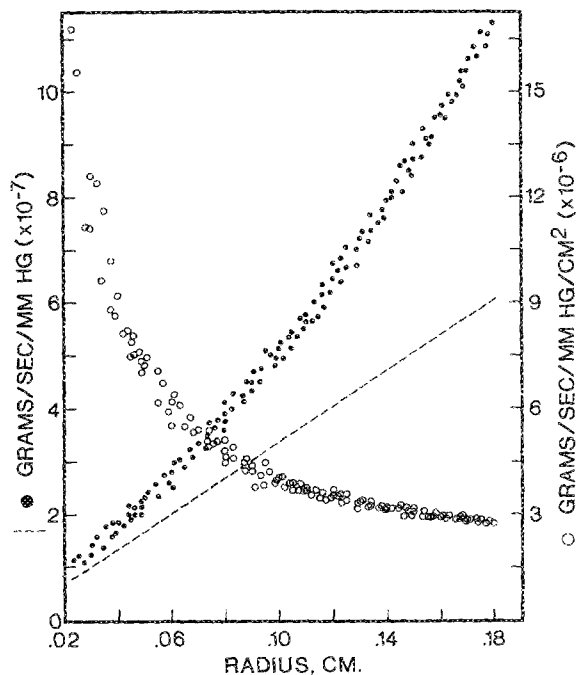


FIG. 2. Closed circles (left ordinate): evaporative rate in g/s/mm Hg vapor pressure as a function of drop radius. Open circles (right ordinate): evaporative rate in g/s/mm Hg vapor pressure/cm² drop area as a function of drop radius. Dashed line (left ordinate): evaporative rate in g/s/mm Hg vapor pressure as a function of drop radius calculated from the Stefan equation.

tors for precise positioning. A fine platinum wire provided electrical connection between the KCl solution and the servo control unit. Another wire connected this unit with the metal base of the hypodermic needle. The microelectrode served as a detector which signals contact or lack of contact with the water drop. When contact is broken, the Inchworm controller is turned on and drives the shaft of the Inchworm translator. This in turn drives the plunger of the Hamilton syringe to add water to the drop. When the drop increases in size to restore contact with the microelectrode, the Inchworm controller is turned off. Cycle time varied from 3 to 10 s. Each pulse generated by the Inchworm controller displaces the shaft of the Inchworm translator by 2 μ m. The rate of pulse generation, and therefore translator shaft displacement, is controllable over a wide range. Drop diameter was kept constant \pm a few μ m. The system was calibrated so that displacement of the Inchworm translator could be expressed in grams of water. The experimental design was to determine evaporative rates in g/s/mm Hg vapor pressure over a range of water drop radii between 0.023 and 0.18 cm. A total of 128 measurements were made. Mathematical analysis was performed using a multiple curve fitting program of 19 different curves.⁷

Figure 2 shows the 128 data points plotted in two ways. Closed circles indicate the relationship of radius and evaporative rate in g/s/mm Hg vapor pressure (left ordinate). Open circles indicate the relationship of radius and evaporative rate in g/s/mm Hg vapor pressure/cm² drop area (right ordinate). The dashed line indicates the relationship of radius and evaporative rate in g/s/mm Hg vapor pressure calcu-

lated from Eq. (2). The curve of best fit for the closed circles, with a correlation coefficient of 0.998, is a parabola:

$$Y = 3.391 \times 10^{-8} + 2.989 \times 10^{-6}X + 1.722 \times 10^{-5}X^2. \quad (4)$$

The curve of best fit for the open circles, with a correlation coefficient of 0.995, is a second-order hyperbola:

$$Y = 1.320 \times 10^{-6} + 2.483 \times 10^{-7}/X + 2.285 \times 10^{-9}/X^2. \quad (5)$$

Several previous studies^{3,5,6} dealt, respectively, with evaporation of water drops, iodine spheres, and drops of organic liquids. In each case the data were reported as a relationship between decreasing surface area or radius against time. From the surface area or radius data it is possible to calculate the change in volume per unit time and plot this against radius. In no case was the relationship linear as predicted by theory, and the data in these studies are reasonably well fit by a parabola.

The data shown in Fig. 2 do not fit the theoretical postulate that evaporative rate is proportional to drop radius. Nor is the evaporative rate proportional to drop surface area, which would result in the open circles lying on a line parallel to the abscissa. As shown in Fig. 2, evaporative rate per cm² surface area does approach an asymptote to the abscissa, and from Eq. (5) the asymptote value is 1.320×10^{-6} g/s/mm Hg vapor pressure/cm². It is difficult to propose a satisfactory explanation for the tremendous increase in evaporative rate per cm² as drop radius decreases. For a drop of 0.023-cm radius to have an evaporative rate of 1.320×10^{-6} per cm², a vapor pressure difference 12.5 times larger than that determined from the drop surface temperature would be required. There is no conceivable way in which this could occur. Woodland and Mack⁶ noted a similar increase in evaporative rate per cm² in their study on very small drops of organic liquids. They postulated that as drop size decreases below 0.1-cm radius, a saturated vapor shell accumulates around the drop. With drops of *n*-dibutyl phthalate ranging from 0.75 to 1.25 μ m radius, they calculated vapor shell thickness in the range of 0.49–0.67 μ m. For drops with radii in the range of 0.023–0.18 cm in this study, the saturated vapor shell thickness would have to range from 0.98 cm at a drop radius of 0.023 cm, to 0.23 cm at a drop radius of 0.18 cm in order to have a constant evaporative rate of 1.320×10^{-6} g/s/mm Hg vapor pressure/cm² for all drop radii. This does not seem reasonable since the temperature of the air surrounding a drop of water increases rapidly within a few millimeters distance from the drop. Therefore, the diffusion coefficient of the water vapor molecules leaving the surface of the drop will increase proportionately. This would not favor accumulation of a saturated vapor shell around the drop. At the present time there seems to be no satisfactory explanation for the observed results of these experiments, which have been carried out with precise control of the parameters involved in accurate determination of evaporative rate, surface temperature, and drop radius.

This work was supported by a grant from the Dean's Research and Education Fund.

¹M. J. Stefan, *Sitzber. Akad. Wiss. Wien II* **65**, 323 (1872).

²I. Langmuir, *Phys. Rev.* **12**, 368 (1912).

³N. Gudris and L. Kulikowa, *Z. Phys.* **25**, 121 (1924).

⁴G. O. Langstroth, C. H. H. Diehl, and E. J. Winhold, *Can. J. Res. A* **28**, 580 (1950).

⁵B. Topley and R. Whytlaw-Gray, *Philos. Mag.* **4**, 873 (1927).

⁶D. J. Woodland and E. Mack, Jr., *J. Am. Chem. Soc.* **55**, 3149 (1933).

⁷W. M. Kolb, *Curve Fitting for Programmable Calculators* (IMTEC, Bowie, MD, 1982).

Scanning tunneling microscope imaging technique for weakly bonded surface deposits

M. H. Jericho and B. L. Blackford

Department of Physics, Dalhousie University, Halifax, Nova Scotia B3H 3J5, Canada

D. C. Dahn

Department of Engineering Physics, Technical University of Nova Scotia, Halifax, Nova Scotia B3J 2X1, Canada

(Received 21 December 1988; accepted for publication 20 February 1989)

An imaging mode for a scanning tunneling microscope is described in which the tunneling needle is periodically withdrawn from the surface under study in order to reduce the elastic interaction effects between needle and substrate during imaging. Examples of images of weakly bonded surface deposits that could not be imaged with the conventional sweep method are presented. The technique also makes it possible to first manipulate and subsequently image deposits that are weakly bonded to a substrate.

The scanning tunneling microscope (STM) has had spectacular success in imaging the surface of inorganic conducting samples and atomic resolution can be obtained for many surfaces.¹ A particularly challenging application of the STM is in the imaging of objects that have been deposited on a flat substrate, such as graphite. Considerable progress has been made in this area and high-resolution images of liquid-crystal molecules, for example, have recently been reported.² A major problem for the imaging of deposits in general is the often poor adhesion of these deposits to the substrate. If imaging is done in air, the inevitable contamination layer between needle and substrate produces needle-substrate interaction forces³ which can cause the needle to push the deposit along the surface rather than image it. This is particularly serious for poorly conducting deposits, such as biological material.⁴

In order to overcome this difficulty and to improve the imaging capability of the STM in the case of weakly bonded surface deposits, we have developed a new operating mode for STM imaging. In the usual operating mode, a constant tunneling current is established and the needle is then scanned in a raster fashion across the surface with the needle hovering at an approximately constant distance over the surface at all times. As a result of needle-deposit interactions, this continuous lateral movement of the needle can result in a sufficiently large buildup of stress that the deposit is dislodged and is moved out of the way. In order to minimize these lateral stresses on the deposit, we use a scanning mode in which the needle is periodically pulled back from the surface and tunneling is interrupted. While the needle is raised, it is moved a short distance along the surface before a new approach is made. A typical needle-stepping cycle is shown

in Fig. 1(a). Trace V_z shows the voltage applied to the z piezo as a function of time. At (1) the needle is withdrawn by lowering the voltage on the z piezo. At (2) the voltage is minimum and the needle is fully withdrawn. The z piezo voltage then remains at that value for about 15 ms and at (3) a new approach is made. As shown on trace I , in Fig. 1(a), the tunneling current during this time is zero. At (4) the approach is complete and tunneling current again flows. The needle withdrawal rate, the time it spends in the fully withdrawn state, the rate at which it returns to the surface, and the length of time the tunneling current flows are all externally controllable. In order to display an image in this mode of operation, the tunneling current is sensed with a boxcar integrator, with the boxcar gate positioned close to the end of the period where the tunneling current flows, in order to allow possible approach transients to die out. The boxcar output is then added to the y -raster voltage and is displayed in the usual way.

For a smooth, triangular x -deflection voltage as used in our study, the needle is still moving while tunneling to the surface is occurring. Because of this, the quality of the image depends on the time the needle spends in the lowered state as well as on the needle velocity over the surface, and it thus depends on the stepping frequency, the x -sweep frequency, and also the steepness of the surface features to be imaged. The lateral movement of the needle during tunneling can, of course, be completely eliminated by using a computer-controlled staircase ramp x deflection instead of the continuous analog sweep used in this study. A computer-controlled scan generator is now being developed for this purpose.

We have imaged steps and surface features on cleaved highly oriented pyrolytic graphite (HOPG) and recorded